

A New Carbon Nanotube-Based Breast Cancer Drug Delivery System: Preparation and In Vitro Analysis Using Paclitaxel

Wei Shao · Arghya Paul · Laetitia Rodes ·
Satya Prakash

Published online: 10 February 2015
© Springer Science+Business Media New York 2015

Abstract Paclitaxel (PTX) is one of the most important drugs for breast cancer; however, the drug effects are limited by its systematic toxicity and poor water solubility. Nanoparticles have been applied for delivery of cancer drugs to overcome their limitations. Toward this goal, a novel single-walled carbon nanotube (SWNT)-based drug delivery system was developed by conjugation of human serum albumin (HSA) nanoparticles for loading of antitumor agent PTX. The nanosized macromolecular SWNT-drug carrier (SWNT-HSA) was characterized by TEM, UV–Vis-NIR spectrometry, and TGA. The SWNT-based drug carrier displayed high intracellular delivery efficiency (cell uptake rate of 80 %) in breast cancer MCF-7 cells, as examined by fluorescence-labeled drug carriers, suggesting the needle-shaped SWNT-HSA drug carrier was able to transport drugs across cell membrane despite its macromolecular structure. The drug loading on SWNT-based drug carrier was through high binding affinity of PTX to HSA proteins. The PTX formulated with SWNT-HSA showed greater growth inhibition activity in MCF-7 breast cancer cells than PTX formulated with HSA nanoparticle only (cell viability of 63 vs 70 % in 48 h and 53 vs 62 % in 72 h). The increased drug efficacy could be driven by

SWNT-mediated cell internalization. These data suggest that the developed SWNT-based antitumor agent is functional and effective. However, more studies for in vivo drug delivery efficacy and other properties are needed before this delivery system can be fully realized.

Keywords Carbon nanotubes · Breast cancer therapy · Paclitaxel · Targeted drug delivery · Human serum albumin

Introduction

Breast cancer is one of the most common causes of death worldwide. It accounts for almost 33 % of all incident cases of cancer in women [1]. Chemotherapy in addition to the primary surgical removal of tumors is a necessary treatment for breast cancer. Widespread use of adjuvant chemotherapy in breast cancer has led to dramatic improvements in survival. Paclitaxel (PTX) is one of the most important antitumor reagents for breast cancer. It promotes microtubule assembly but prevents its disassembly, and therefore, it disturbs the important cellular functions of microtubule, including mitosis, cell transport, and cell motility. Since the drug is not specific for cancer cells, it affects all fast dividing cells [2], therefore, it causes severe side effects [3, 4]. In addition, due to the poor solubility of the drug, it is necessary to use organic solvent such as cremophor, which causes hypersensitivity reactions [5, 6]. The commercial PTX formulation, Taxol[®], has to be infused intravenously over a long period of time. Abraxane[®], a human serum albumin (HSA) nanoparticle formulated PTX, has been developed to solve the problems of PTX. This formulation showed improved drug efficacy compared with solvent formulated PTX, however, the side effects still persist [7–9].

W. Shao · L. Rodes · S. Prakash (✉)
Biomedical Technology and Cell Therapy Research Laboratory,
Department of Biomedical Engineering, Faculty of Medicine,
McGill University, 3775 University Street, Montreal,
QC H3A 2B4, Canada
e-mail: satya.prakash@mcgill.ca

A. Paul
Department of Chemical and Petroleum Engineering, University
of Kansas, Learned Hall 1530 W 15th St, Lawrence, KS 66045,
USA

An effective cancer delivery system should be able to specifically deliver chemotherapy drugs to tumor tissues in order to reduce off-target toxicity. In addition, it is preferentially able to carry drugs inside of cells to take effect. Nanoparticles have been shown to accumulate in tumor tissues. This is due to the leaky tumor vasculature permeable to nanoparticles. The phenomenon is termed as tumor-selective enhanced permeation and retention (EPR) effect. The EPR effect is the basis for design of nanoparticle therapeutic for selective targeting tumors.

Carbon nanotube (CNT), discovered by Iijima in 1991, is a novel-type synthetic nanomaterials with distinct hollow, cylindrical structure. CNT can be viewed as rolled from layers of graphene sheets. They can be one layer (single-walled nanotubes SWNT) or multiple layers (multi-walled nanotubes MWCNT). CNT possesses many interesting properties as drug carriers, such as, specific optical characteristics for *in vivo* detection and imaging; needle-like structure for loading large amount of payloads along the longitude without the constraint of the volume. In addition, CNT can easily enter all sorts of cells, including mammalian, yeast, and bacteria cells [10]. Biodistribution studies have shown high tumor accumulation of functionalized SWNT [11]. Inspired by these findings, CNT has been widely investigated for delivery of antitumor agents, including DNA [12, 13], siRNA [14, 15], peptides [16], and drugs [17]

Since CNT consists of the supramolecular structure that is formed by covalent bonding between carbon atoms, the drug loading to this pre-formed structure is very challenging. Owing to the hollow structure of nanotubes, small molecule drugs can be loaded into the interior of CNT through a simple capillarity-induced filling, however, the loading amount is very low [18]. Researchers have also found that CNT contains large surface area that allows direct absorption of some hydrophobic drugs, preferably the drug molecules that contain flat, benzene ring structure, e.g., doxorubicin [19]. However, for drugs with bulky structures, e.g. PTX, no effective drug-loading scheme is available.

To improve loading efficiency of PTX to CNT, in this study, we have developed a HSA nanoparticle conjugated SWNT for intracellular delivery of PTX. The design is based on the property of high binding affinity of PTX to HSA [20], which is the most abundant plasma protein that acts as carriers in blood for certain molecules with poor water solubility, such as long chain fatty acid, metal ions, and some drugs [21]. It was hypothesized that HSA could be used as a platform for loading of PTX onto SWNT. In this study, an efficient SWNT-based, HSA nanoparticle conjugated drug delivery system has been developed, which provides a new scheme for effective loading of PTX to SWNT.

Materials and Methods

Noncovalent Functionalization of SWNT with PL-PEG-NH₂

Noncovalent functionalization of SWNT (HiPco, Unidym Inc, USA) was prepared by modified method as previously described [22]. The SWNT was firstly dispersed in organic solvent DMF by sonication for 5 min in a bath sonicator (model 2510, Branson Ultrasonics, CT) at a concentration of 2 mg/ml. The amphiphilic lipid polymer, phospholipid polyethylene glycol (PL-PEG-NH₂, 2 K Da, Avanti Lipid company, USA) was dissolved in deionized (DI) water at a concentration of 2 mg/ml. Ten times of volume of PL-PEG-NH₂ water solution was dropwisely added to the solvent-dispersed SWNT. The mixture was sonicated for 1 h at room temperature with changing water every 20 min to avoid overheating. After sonication, the suspension was centrifuged at 17,500 rpm (50Ti, Beckman Coulter, USA) for 6 h at room temperature to remove SWNT bundles and impurities in the precipitation. Excess PL-PEG-NH₂ was removed by three times of washing using centrifugation filtration units (100 kDa cutoff) before use.

Quantification of SWNT by UV–Vis–NIR Spectroscopy

UV–Vis–NIR spectra of PL-PEG-NH₂ functionalized SWNT were measured with 1 cm quartz cuvettes using UV–Vis–NIR spectrophotometer (Cary-100 bio, Varian Inc) over the range of 200–850 nm. The extinction coefficient was obtained by plotting the absorbance at 565 nm against SWNT concentration (mg/l) and subsequent linear regression analysis.

Thermogravimetric Analysis (TGA)

TGA was performed using TGA Q500 (TA instruments Ltd, UK). Samples were loaded in the sample holder and the materials were heated up at a rate of 10 °C/min up to 800 °C under nitrogen. The weight loss and derivative weight were recorded continuously.

Transmission Electron Microscopy (TEM)

The size and shape of functionalized SWNT and the SWNT-HSA conjugation were examined by TEM (Phillips169 CM200 200 kV). 5 µl of sample solution was deposited on carbon-coated copper grid and allowed to dry for 10 min. The excess liquid on grid was removed by touching the edge of the grid with filter paper.

Cell Culture

MCF-7 breast cancer cells (ATCC) were maintained in Dulbecco's modified Eagle's Medium (DMEM, Invitrogen, Canada) supplemented with 10 % fetal bovine serum (Invitrogen, Canada). The cells were cultured in a humidified incubator with 5 % CO₂ at 37 °C.

Labeling SWNT with Fluorescent Dye FITC and Cell Internalization Assay

Fluorescent SWNT was prepared either by covalently linking fluorescein isothiocyanate (FITC) to PL-PEG-NH₂ for coating of SWNT, or noncovalently loading FITC directly on sidewall of nanotubes. For covalent labeling, FITC was conjugated to PL-PEG-NH₂ via its isothiocyanate group (–N=C=S) reacting with amino group in PL-PEG-NH₂ [22]. In general, 10 mg of PL-PEG-NH₂ was dissolved in 5 ml of 0.1 M NaHCO₃–Na₂CO₃ buffer solution (pH 9.0), and 100 µl of 13 mM FITC was added and incubated at room temperature in dark for one overnight. For noncovalent loading FITC on nanotubes, SWNT were firstly mixed with FITC in organic solvent DMF with 5 min of sonication in a water bath, and then noncovalently functionalized by PL-PEG-NH₂ followed by further conjugation of HSA nanoparticles to PL-PEG-NH₂. The excess FITC was removed by dialysis using membrane cassette with 100 kDa cutoff.

For cell penetration assay, the MCF-7 cells were seeded in 96-well plate at a density of 2×10^4 cells/well in 200 µl medium at one night before the assay. The cells were incubated with FITC labeled SWNT at a concentration of 1–5 µg/ml (equivalent of SWNT amount) for 24 h. The cells were washed and viewed under fluorescence microscope.

Preparation of HSA Nanoparticles by Crosslinking of Protein

The HSA nanoparticles were prepared by crosslinking of HSA proteins using EDC (Thermo Scientific), plus sulfo-NHS (Thermo Scientific) as crosslinking reagents following the handbook provided by the manufacture. Briefly, EDC (30 mM) and sulfo-NHS (5 mM) were added dropwisely to 10 ml of HSA (20 mg/ml) in PBS buffer (pH 7.4). The mixture was incubated at room temperature for 2 h with shaking. The generated HSA nanoparticles were purified by washing three times with PBS using centrifugation filtration units (100 kDa cutoff).

Conjugation of HSA Nanoparticles to SWNT-PL-PEG

Heterobifunctional linker molecule, NHS-PEG₄-Maleimide (SM(PEG)₄, Thermo Scientific) was used for linking HSA

to PL-PEG-NH₂ functionalized SWNT according to manufacturer's instruction. The conjugation reaction carried out in three steps. Briefly, the first step was linking SM(PEG)₄ to the amino end of PL-PEG-NH₂ that was coated on SWNT. 5 ml of SWNT/PL-PEG-NH₂ in PBS buffer (pH 7.4) mixed with 8 µl of 250 mM SM(PEG)₄, and incubated at 4 °C for 2 h, and then the excess linking molecules were removed by washing with PBS using centrifugation filtration unit (100 kDa cutoff). The second step was to activate sulfhydryl group in HSA by Traut reagents (Sigma). 20 ml of HSA nanoparticles (5 mg/ml) in PBS buffer (pH 7.4) mixed with 100 µl of Traut reagent (50 mM), and 100 µl EDTA (0.5 M), and then incubated at room temperature for 1 h. The excess reagents were removed by washing with PBS using centrifugation filtration unit. In the third step, the SWNT/PL-PEG-NH₂-SM(PEG)₄ mixed with sulfhydryl group activated HSA, and incubated at room temperature for 30 min. The SWNT-HSA conjugates were purified by washing three times with DI H₂O using centrifugation filtration unit (100 kDa cutoff). The dry SWNT-HSA can be obtained by freeze-drying process.

Loading of PTX onto SWNT-HSA and Quantification of PTX Solution

Loading of PTX onto SWNTs-HSA followed the procedure developed by Lay et al. [23] with modifications. Briefly, PTX was firstly dissolved in methanol at a concentration of 4 mg/ml. SWNT-HSA dry powder was added to PTX methanol solution at a concentration of 15 mg/ml and sonicated for 30 min, and then, large amount of DI water were dropwisely added to the SWNT-HSA/PTX methanol solution up to ten times of its original volume with sonication. After water addition process, the solution was sonicated for additional 1 h. During sonication process, ice was added to sonication bath every 20 min to prevent overheating. The solution was equilibrated at room temperature for one overnight, then the excess unbound PTX precipitated from solution. The supernatant containing SWNT-HSA/PTX was transferred to a fresh tube. The unbound PTX in precipitates was extracted with dichloromethane, and then dried under vacuum hood. The extracted PTX was re-dissolved in methanol for quantification by UV spectrometry using established standard curve at 228 nm.

Cell Viability Assay

Cell viability was evaluated in MCF-7 breast cancer cells by MTS assay using the Cell Titer 96[®] Aqueous Non-Radioactive Cell Proliferation MTS Assay kit (Promega). Briefly, triplicates of 1×10^4 /well in 96-well plates were treated with different PTX formulations at 37 °C for varied

time period. MTS assay followed manufacturer's instructions. The 3-(4,5-dimethylthiazol-2-yl)-5-(3-carboxymethoxyphenyl)-2-(4-sulfophenyl)-2H-tetrazolium (MTS) was reduced to form formazan by mitochondrial enzyme dehydrogenase present in viable cells and the formazan concentration in cell culture was measured at absorbance of 490 nm using 1420-040 Victor3 Multilabel Counter (Perkin Elmer, USA). The amount of formazan is proportional to the number of viable cells. Cell viability was calculated as the percentage of viable cells relative to that in untreated control group.

Detection of Apoptosis by TUNEL Staining

The TUNEL staining of apoptotic cells upon drug treatments was performed using the DeadEnd Colorimetric TUNEL System (Promega) according to the manufacturer's instruction. TUNEL detects DNA fragmentation (an indicator of apoptosis) of cells undergoing apoptosis. The ends of fragmented DNA are labeled by a modified TUNEL (TdT-mediated dUTP Nick-End Labeling). The terminal deoxynucleotidyl transferase (TdT) enzyme adds a biotinylated nucleotide at the 3'-OH ends of fragmented DNA; the biotinylated nucleotides are conjugated with horseradish-peroxidase-labeled streptavidin. The peroxidase is then detected using its substrate, hydrogen peroxide, and the chromogen, diaminobenzidine. The nuclei of apoptotic cells are stained brown.

Statistical Analysis

Statistical analysis was carried out using SPSS software (Minitab Inc, State College, PA). Data were expressed as mean \pm standard deviation (SD). Statistical significance was accepted at a level of $p < 0.05$. Differences between the groups were tested through analysis of variance, and Tukey's post hoc analysis was applied to detect the difference between the groups.

Results

Design of SWNT-Based Drug Delivery System for PTX

In this study, a CNT-based drug delivery system has been designed and developed by conjugation of HSA nanoparticles to SWNT for delivery of cancer drug PTX. As illustrated in Fig. 1, SWNT, dispersed via a lipid-polymer PL-PEG-NH₂, served as a drug-loading platform, on which, cross-linked HSA nanoparticles were conjugated to amino end group of PL-PEG-NH₂ for PTX loading. Both noncovalent and covalent chemical approaches were

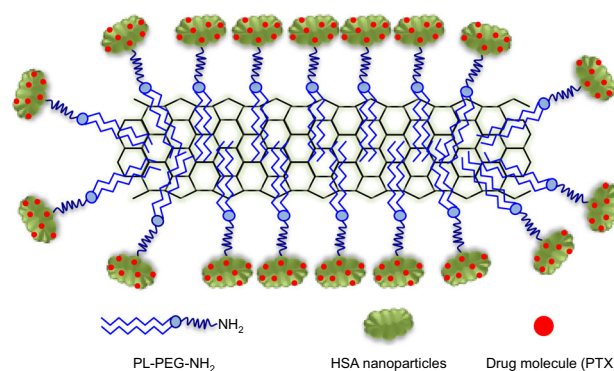


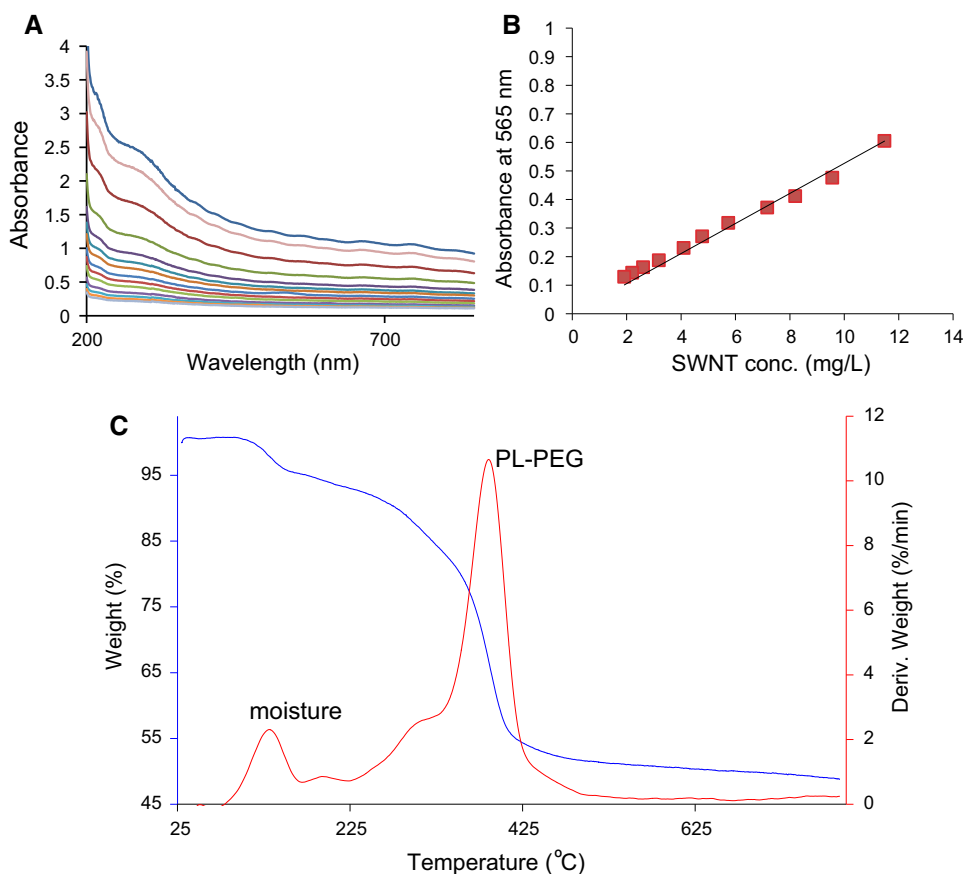
Fig. 1 Schematics of human serum albumin (HSA) nanoparticle conjugated to single-walled carbon nanotubes (SWNT) for delivery of cancer drug paclitaxel (PTX). SWNT is dispersed in water solution via a lipid-polymer PL-PEG-NH₂, and served as a drug-loading platform, on which, cross-linked HSA nanoparticles were conjugated to amino end group of PL-PEG-NH₂ for loading cancer drug PTX. Both noncovalent and covalent chemical approaches were applied to construct the SWNT-based drug delivery system. PL-PEG-NH₂ was coated on SWNT surface through hydrophobic interaction as to disperse SWNT in aqueous solution. HSA was chosen as an adapter for PTX loading due to its high binding affinity to PTX. It is expected that the nanosized macromolecular structure of the delivery system could favor the accumulation of the cancer drug in tumor tissues by EPR effect, and cellular uptake of drug could be driven by the needle-like CNT

applied to build the SWNT-based drug delivery system. PL-PEG-NH₂ was coated on SWNT surface via hydrophobic interaction to disperse SWNT in aqueous solution. HSA was chosen as an adapter for drug loading due to its high binding affinity to PTX [20]. PTX can be loaded on SWNT-HSA via the strong HSA-PTX association. It is expected that the nanosized macromolecular structure of the delivery system could favor the accumulation of the cancer drug in tumor tissues by EPR effect, and cellular uptake of the drug could be driven by the needle-like structure of SWNT.

Preparation of SWNT-HSA and the Structural Characterization

The raw HiPco SWNT was firstly noncovalently functionalized by PL-PEG-NH₂. The amino functional end group of the PL-PEG was used for further conjugation of HSA. The PL-PEG-NH₂ functionalized SWNT was very stable in water, PBS, and cell culture medium. The dry SWNT-PL-PEG-NH₂ samples can be easily re-dispersed in aqueous solution with 5 min of sonication after storing at room temperature for at least 3 months. The SWNT solution displayed strong absorption along UV-NIR region, which was used for quantification of SWNT (Fig. 2a). The mass extinction coefficient of the SWNT solution was determined as 0.0527 mg l⁻¹ cm⁻¹ by plotting the absorbance at 565 nm (Fig. 2b). TGA was applied to evaluate the content of

Fig. 2 In vitro characterization of the SWNT dispersed in PL-PEG-NH₂ (SWNT-PL-PEG). **a** UV-Vis spectra of SWNT-PL-PEG-NH₂ at various concentrations. **b** Absorbance at 565 nm vs. SWNT concentration, *solid line* is Beer's law fit to obtain mass extinction coefficient of SWNT $\epsilon = 5.27 \times 10^{-5} \text{ g}^{-1} \text{ cm}^{-1}$ **c** Thermogravimetric analysis (TGA) of SWNT-PL-PEG. The weight loss before 150 °C (around 5 %) was due to moisture of SWNT-PL-PEG sample. The PL-PEG content absorbed on SWNT was 55 % (w) (the percentage PL-PEG was re-calculated by subtracting the weight of moisture from the sample)



PL-PEG-NH₂ coated on SWNT, since SWNT is stable up to 1,000 °C, and PL-PEG-NH₂ can be fully degraded from 200–500 °C under nitrogen condition. Our TGA result in Fig. 2c showed two peaks in derivative weigh loss. The weight loss before 150 °C (around 5 %) was due to moisture in SWNT-PL-PEG sample. By subtracting the weight of moisture from the sample, PL-PEG contents coated on SWNT was calculated as 55 % (w). The high coverage of PL-PEG-NH₂ on SWNT could explain the stability of PL-PEG functionalized SWNT in aqueous solution.

To prepare SWNT-HSA conjugates, the HSA was firstly crosslinked to form nanoparticles. In order to obtain HSA nanoparticles with small size, short linker molecules, EDC, and sulfo-NHS were used. With the conjugation condition described in materials and methods section, homogenous, small HSA nanoparticles were generated. The diameter of HSA nanoparticles was 60.4 ± 1.1 nm as revealed by particle size analyzer. The size and morphology of HSA nanoparticles were confirmed by TEM (Fig. 3c). SWNT-HSA was obtained by further conjugation of HSA nanoparticles to SWNT via heterobifunctional linker molecules. TEM image of SWNT-HSA showed that HSA nanoparticles were densely arranged on sidewall of CNT, suggesting that large surface area for PTX loading could be achieved by the SWNT-HSA drug carrier (Fig. 3b).

Investigation of Intracellular Delivery Efficiency of SWNT-HSA Drug Carrier

Since it is expected that the SWNT-HSA drug carrier could carry drugs into cells and take effects inside of cancer cells, the cellular internalization of SWNT-HSA was investigated. For cell internalization assay, fluorescent dye FITC was used to label SWNT-HSA. We firstly tried to conjugate FITC to HSA to make fluorescent nanoparticles. However, FITC-conjugated HSA spontaneously formed the particles up to 500 nm as measured by particle size analyzer. The formation of the big nanoparticles was possibly due to aggregation of HSA through the hydrophobic FITC molecules. Because the size of FITC-conjugated HSA particles was too big even before crosslinking, we then changed to label SWNT-HSA by adsorption of the flat benzene-containing FITC on sidewall of SWNT. The formation of SWNT-HSA/FITC complex was confirmed by dialysis procedure using a membrane cassette of 100 kDa cutoff, in which, yellowish FITC remained with SWNT-HSA even with repeated changing water for 2 days. Cell internalization of SWNT-HSA/FITC was examined using MCF-7 cells. After the cells were incubated with 1–5 µg/ml (equivalence of SWNT amount) of SWNT-HSA/FITC for 24 h,

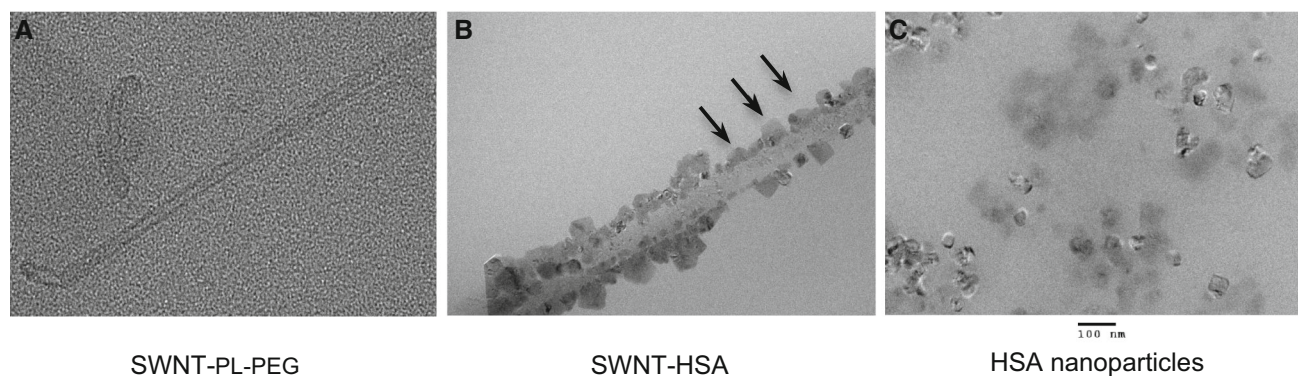


Fig. 3 Characterization of SWNT-HSA drug carriers by transmission electron microscopy (TEM). **a** SWNT-PL-PEG-NH₂, **b** SWNT-HSA, **c** HSA nanoparticles. HSA nanoparticles were conjugated to SWNT-PL-PEG-NH₂ via heterobifunctional linker molecule NHS-PEG₆-

maleimide SM(PEG)₆. 5 μ l of samples deposited to copper grid and viewed under TEM (200 kV). *Arrowheads* indicate HSA nanoparticles conjugated to SWNT-PL-PEG-NH₂

it was obtained percentage of FITC internalization of 72, 80, and 81 % for 1, 2.5, and 5 μ g/ml of SWNT-HSA/FITC, respectively, indicating that the SWNT-HSA drug carriers could be very efficient in carry drugs into cancer cells (Fig. 4).

Examination of Cytotoxicity of the SWNT-HSA Drug Carrier

The toxicity of SWNT-HSA drug carrier was examined using MCF-7 cells. The cells were treated with varied amounts of SWNT-HSA in range of 1–10 μ g/ml (equivalent of SWNT concentration) for 24 h, and the cell viability was examined by MTS assay. Cell viability in untreated group was assigned as 100 % and its O.D from MTS assay was used to calculate normalized cell viability in other groups. Result showed, at treatment dosage of less than 5 μ g/ml, the cell viability was larger than 90 %; at maximum dosage tested (10 μ g/ml), cell viability was 85 % (Fig. 5). So, the toxicity of SWNT-HSA was minor, and therefore it is suitable for drug delivery applications.

Evaluation of SWNT-HSA Drug Formulation and its Stability

Since the water solubility of PTX is very low (\sim 0.4 μ g/ml), it is not possible to load PTX to SWNT-HSA directly in aqueous solution. In order to load PTX on SWNT-HSA, we firstly dissolved PTX in methanol in high concentration, then, the dry SWNT-HSA was added in the methanol solution and dispersed by sonication. It was observed that SWNT-HSA was well dispersed in methanol. In the next step, large amount of DI water were dropwisely added to the SWNT-HSA/PTX methanol solution with sonication. During this process, the hydrophobic interaction would allow binding of PTX to SWNT-HSA. After water addition

process, the mixture was continuously sonicated for 1 h in order to fully disperse the SWNT-HSA/PTX in water–methanol solution. The obtained SWNT-HSA/PTX water–methanol solution was equilibrated at room temperature for one overnight to allow precipitation of unbound PTX. In the next day, it was observed that some solid precipitated from solution. The supernatant containing soluble SWNT-HSA/PTX was carefully transferred to a fresh tube, and then washed three times to remove methanol and concentrate to its initial volume using centrifugation filtration units (100 kDa cutoff). The PTX in precipitation was extracted by dichloromethane for determination of its quantity by UV spectrometry using established standard curve of PTX at 228 nm. The PTX concentration in SWNT-HSA solution was calculated indirectly by subtracting the precipitated PTX from the total amount of the PTX added. By this way, we calculated the concentration of SWNT-HSA/PTX in solution to be 2.71 mg/ml (equivalent of PTX), which was 7,000 times more soluble in water than free PTX. The PTX-loaded SWNT-HSA was stable without apparent PTX precipitation after for at least 1 month.

Investigation of Antitumor Effect of SWNT-HSA Formulated PTX

The antitumor effect of SWNT-HSA/PTX was investigated in breast cancer cell line MCF-7. Free PTX (in methanol) and HSA nanoparticle bound PTX (HSA/PTX) were used to compare the drug effects. The results in Fig. 6 showed that, within 72 h of drug treatment, free drug PTX dissolved in methanol showed slightly higher level of cell growth inhibition than HSA/PTX and SWNT-HSA/PTX, however the delivery vehicle methanol alone caused 12–14 % cell death. Between HSA/PTX and SWNT-HSA/PTX groups, there was little difference in cell viability

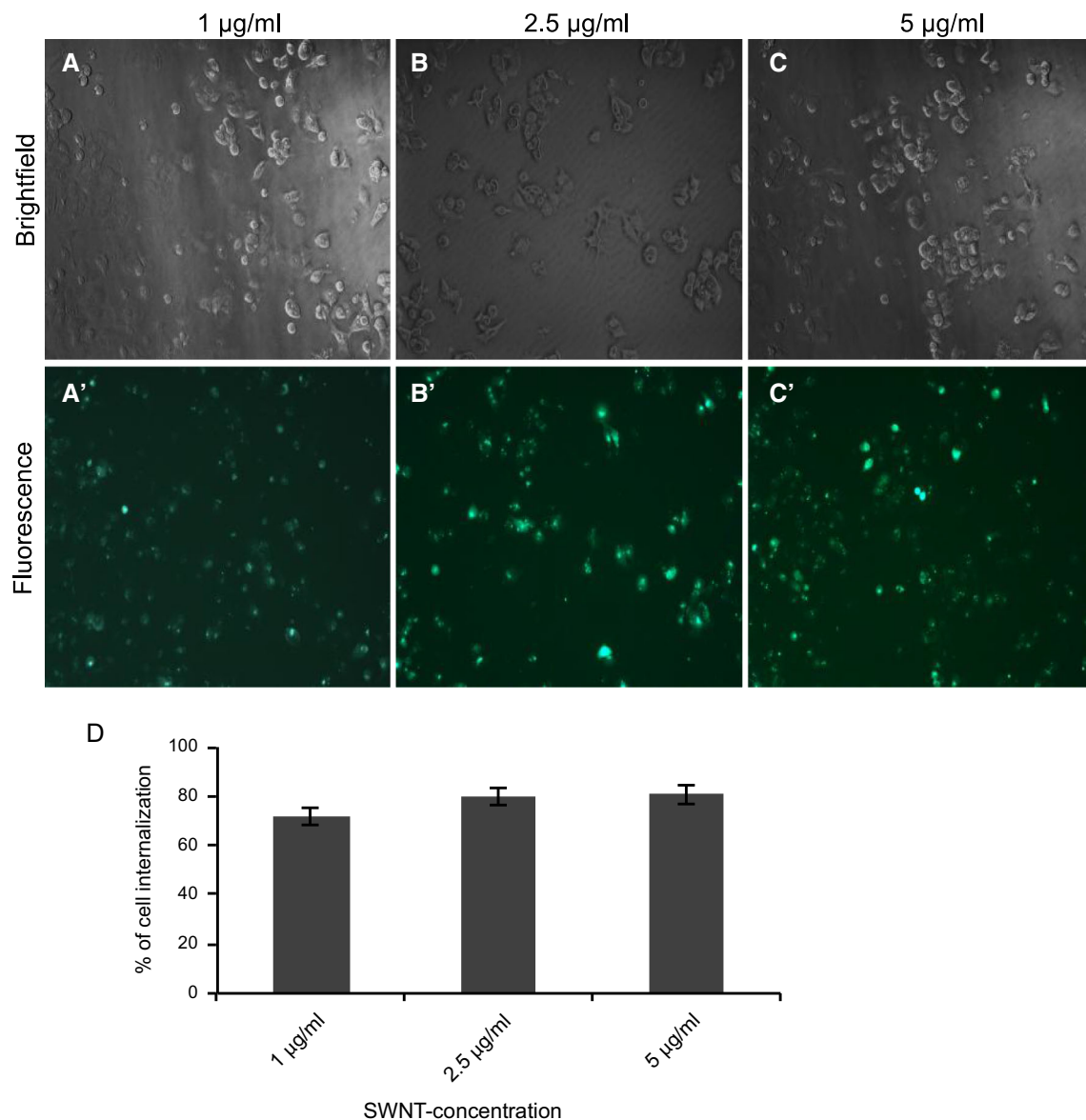


Fig. 4 SWNT-HSA drug carrier intracellular drug delivery efficiency evaluated by cell internalization assay. **a–c** Microscopic image of MCF-7 cells incubated with fluorescent dye labeled SWNT-HSA at amount of 1, 2.5, and 5 µg/ml of SWNT-HSA/FITC, respectively. **d** Percentage of cell internalization evaluated by cell counting. The cells were incubated with 1–5 µg/ml (equivalence of SWNT amounts)

within 24 h of drug treatment, however, after 48 h of drug incubation, SWNT-HSA/PTX demonstrated stronger cell growth inhibition than HSA/PTX (cell viability of 63 vs 70 % in 48 h and 53 vs 62 % in 72 h).

It is known that PTX induces apoptosis in cells by microtubule disruption. Apoptosis induced by different PTX formulations was examined using TUNEL (TdT dUTP nick-end labeling) staining. TUNEL staining showed that apoptotic cells were detected with all three PTX formulations (Fig. 7). By counting the number of TUNEL-positive cells, it was obtained that the ratio of apoptotic

of SWNT-HSA/FITC for 24 h, and then the cells were washed and viewed under fluorescence microscope. The percentage fluorescence positive MCF-7 cells were determined by counting the cell numbers in five randomly selected views under microscope. The percentages of cell internalization were 72, 80, and 81 % for 1, 2.5, and 5 µg/ml of SWNT-HSA/FITC, respectively

cells was in range of 7–8 % for all three PTX formulations and there was no statistic significance between them, suggesting the same mechanism of drug action could be responsible for all three PTX formulations.

Discussions

As fast growing tissues, tumors display enhanced vascular permeability due to high demand for nutrients and possibly oxygen. The poorly aligned, defective endothelial layer is one

of the most important features for tumor vasculature. Nanoparticles have been found to accumulate in tumor tissue due to EPR effect, which has been observed for large proteins,

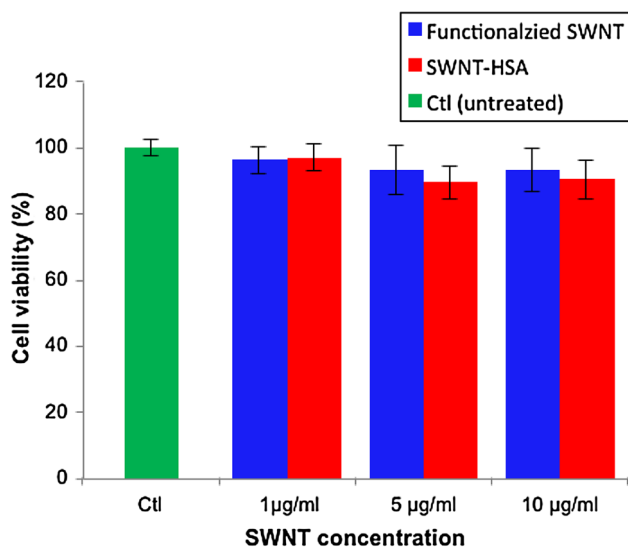


Fig. 5 Investigation of SWNT-HSA cytotoxicity in breast cancer cell line. MCF-7 cells were incubated with SWNT-HSA at different SWNT concentrations for 24 h. Cell viability was measured MTS assay. Cell viability in untreated control was assigned as 100 % and its O.D from MTS assay was used to calculate cell viability in test groups. With tested dosage (<10 µg/ml), The toxicity in both functionalized SWNT and SWNT-HSA was minor (cell viability >85 %) compared with that in control group

polymers, and lipids in a variety of experimental and human solid tumors [24]. The EPR effect is the basis for design of nanoparticle drugs for selective targeting to tumors. Small molecule drugs can be conjugated to nanoparticles for specifically targeting tumor tissues, thus minimize their system toxicity. In this study, we have successfully constructed a novel needle-like SWNT-HSA carrier for delivery of PTX. We have shown that SWNT-HSA can carry payloads to cancer cells, and therefore, they are excellent intracellular drug carrier for potential system delivery.

Because of high binding affinity of HSA to PTX, we have selected HSA protein as an adapter for loading drug PTX to CNTs. As we know, HSA is an endogenous protein and present in large amount in blood, and is therefore nonimmunogenic, nontoxic, and biodegradable. Conjugation of HSA on the surface of CNTs could prevent CNTs from elimination by immune system.

The in vitro drug efficacy of SWNT-HSA/PTX was compared to free drug (in methanol) and HSA/PTX using breast cancer cell line MCF-7 cells. With drug treatment amount of 10 ng/ml, we observed free drug caused more cell death than HSA/PTX and SWNT-HSA/PTX, however, methanol alone caused significant level of cell death (around 14 %). Both nanoparticle PTX formulations, SWNT-HSA/PTX and HSA/PTX, could remove toxic solvent, and therefore, could reduce side effects in system delivery. In our experiment, the SWNT-HSA/PTX drug arrived the same level of cell growth inhibition as that of free drug after 72 h of drug incubation. The delayed drug

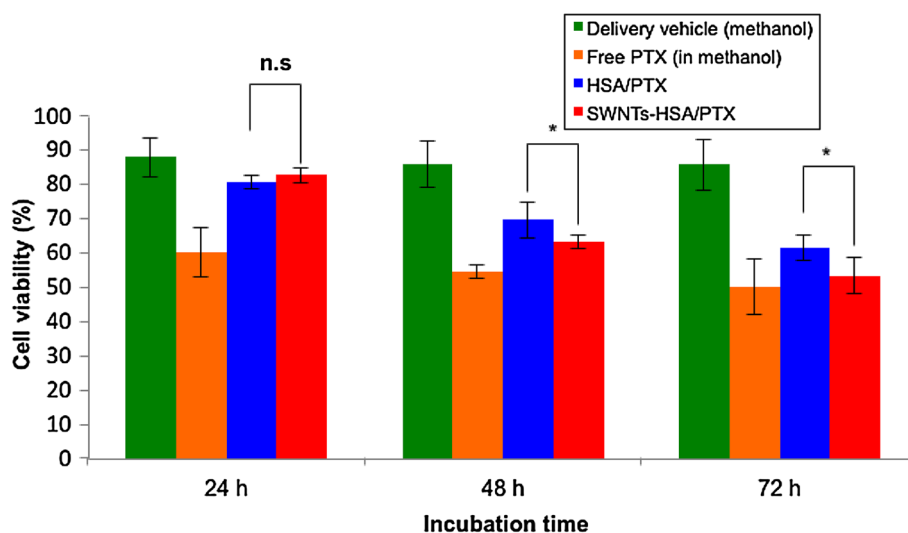


Fig. 6 In vitro antitumor effect of SWNT-HSA/PTX formulation with time. MCF-7 cells were treated with 10 ng/ml (equivalent of PTX) in PTX/methanol, HAS/PTX, or SWNT-HSA, respectively, for 24–72 h. Cell viability was measured by MTS assay. Cell viability in untreated control was assigned as 100 % and its O.D from MTS assay was used to calculate cell viability in test groups. Within 72 h of drug treatment, free drug PTX dissolved in methanol showed slightly higher level of cell growth inhibition than HSA/PTX and SWNT-

HSA/PTX, however the delivery vehicle methanol alone caused 12–14 % cell death. Between HSA/PTX and SWNT-HSA/PTX groups, there was little difference in cell viability within 24 h of drug treatment, however, after 48 h of drug incubation, SWNT-HSA/PTX demonstrated stronger cell growth inhibition than HSA/PTX (cell viability of 63 vs 70 % in 48 h and 53 vs 62 % in 72 h). Asterisk indicates statistically significant difference between two groups; *ns* indicates no statistically significance, $p < 0.05$ ($n = 3$)

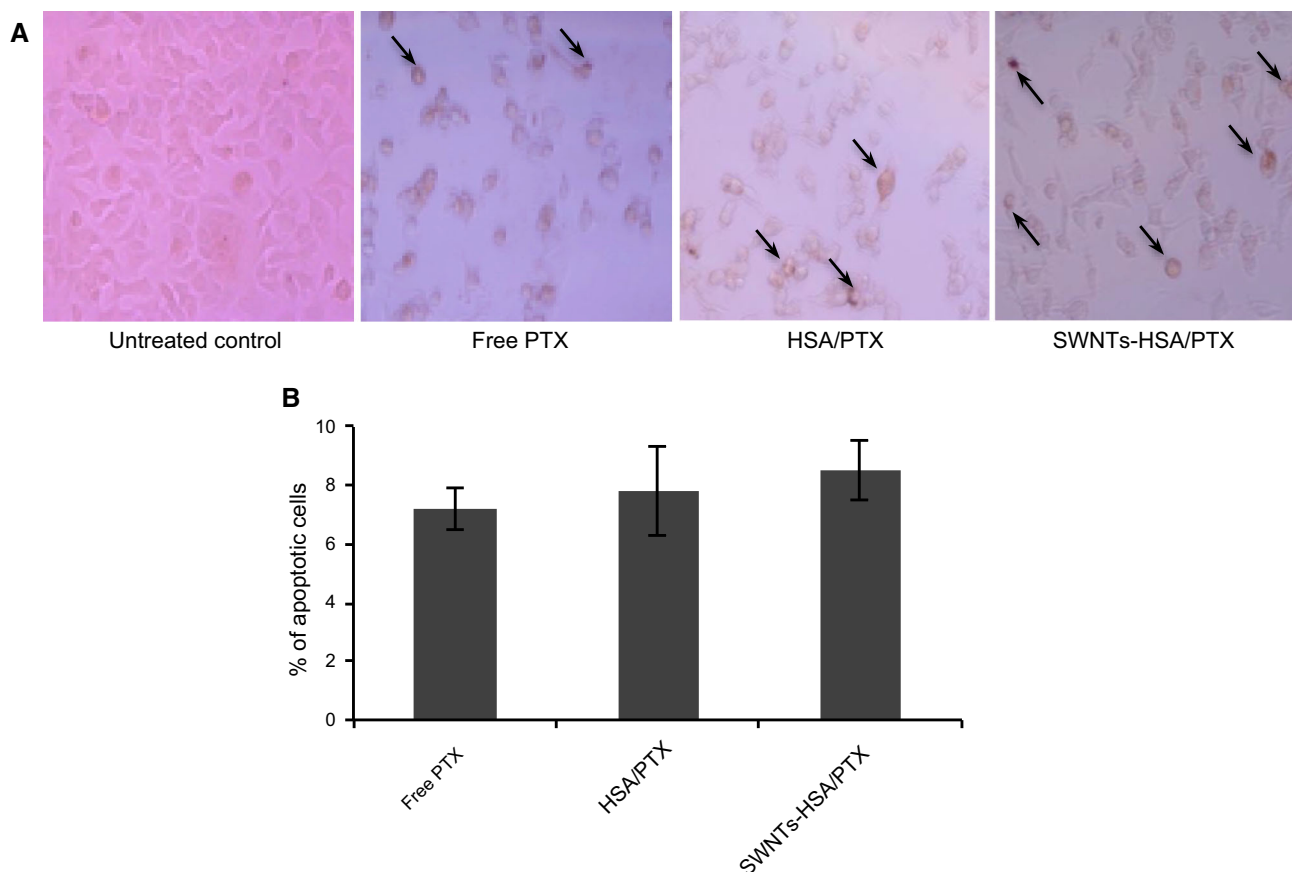


Fig. 7 Apoptotic effect of SWNT-HSA/PTX formulation on breast cancer cells as analyzed by TUNEL staining. **a** Microscopic image of TUNEL staining of MCF-7 cells treated with free PTX, HSA/PTX, and SWNT-HSA/PTX **b** the percentage of apoptotic cells detected with TUNEL staining. MCF-7 cells were treated with 10 $\mu\text{g}/\text{ml}$ (equivalent of PTX) in PTX/methanol, HSA/PTX, or SWNT-HSA/

PTX, respectively, for 48 h. The apoptotic cells were stained in dark brown. By counting the number of TUNEL-positive cells in five randomly selected views under microscope, the obtained percentage of apoptotic cells were 7.2, 7.8, and 8.5 % for free PTX, HSA/PTX, and SWNT-HSA/PTX, respectively. *Arrowheads* indicate the apoptotic cells

effect could be due to slow release of PTX from SWNT-HSA, since only unbound PTX is pharmacologically active. By comparing drug efficacy between HSA/PTX and SWNT-HSA/PTX, we showed that the SWNT-HSA/PTX achieved slightly higher antitumor effect than HSA/PTX. The enhanced toxicity could be driven by SWNT-mediated internalization of the HSA/PTX into the cells.

Conclusions

In this study, a novel HSA nanoparticle conjugated SWNT was developed for intracellular delivery of PTX for treatment of breast cancer. The SWNT-HSA drug carrier possesses nanosized macromolecular structure and it also demonstrated excellent intracellular drug delivery efficiency. The SWNT-HSA/PTX formulation enables removal of organic solvent, and therefore, the toxic effects due to the

organic solvent can be avoided. The SWNT-HSA formulated PTX displayed stronger antitumor effect than HSA nanoparticle formulated PTX. The increased cancer cell inhibition effect could be driven by SWNT-mediated cell internalization. Thus, SWNT-HSA drug carrier is very promising for specifically delivery of PTX to cancer cells, thus, it is worthy for further in vivo applications.

Acknowledgments This work is supported by research grant to Satya Prakash from Canadian Institutes of Health Research (CIHR) (MOP 93641). W. Shao acknowledges the Excellence Award from Biomedical Engineering Department, McGill University and the financial support from FRQS (Fonds de recherche du Québec—Santé) Doctoral award. L. Rodes acknowledges the financial support from FRQS (Fonds de recherche du Québec—Santé) Doctoral award. A. Paul acknowledges the Alexander Graham Bell Post Graduate Scholarship-Doctoral from Natural Sciences and Engineering Research Council of Canada (NSERC). The authors are grateful for the assistance provided for transmission electron microscopy imaging by Xue-Dong Liu, Department of Physics, McGill University.

References

1. Lester, J. (2007). Breast cancer in 2007: Incidence, risk assessment, and risk reduction strategies. *Clinical Journal of Oncology Nursing*, *11*(5), 619–622.
2. Rowinsky, E. K., et al. (1993). Clinical toxicities encountered with paclitaxel (Taxol). *Seminars in Oncology*, *20*(4 Suppl 3), 1–15.
3. Kavallaris, M., Verrills, N. M., & Hill, B. T. (2001). Anticancer therapy with novel tubulin-interacting drugs. *Drug Resistance Updates*, *4*(6), 392–401.
4. Eniu, A., Palmieri, F. M., & Perez, E. A. (2005). Weekly administration of docetaxel and paclitaxel in metastatic or advanced breast cancer. *The Oncologist*, *10*(9), 665–685.
5. Sun, M., et al. (2010). Treatment of metastatic renal cell carcinoma. *Nature Reviews Urology*, *7*(6), 327–338.
6. Menard-Moyon, C., et al. (2010). Functionalized carbon nanotubes for probing and modulating molecular functions. *Chemistry & Biology*, *17*(2), 107–115.
7. Gardner, E. R., et al. (2008). Randomized crossover pharmacokinetic study of solvent-based paclitaxel and nab-paclitaxel. *Clinical Cancer Research*, *14*(13), 4200–4205.
8. Gradishar, W. J., et al. (2005). Phase III trial of nanoparticle albumin-bound paclitaxel compared with polyethylated castor oil-based paclitaxel in women with breast cancer. *Journal of Clinical Oncology*, *23*(31), 7794–7803.
9. Davis, M. E., Chen, Z. G., & Shin, D. M. (2008). Nanoparticle therapeutics: an emerging treatment modality for cancer. *Nature Reviews Drug Discovery*, *7*(9), 771–782.
10. Kostarelos, K., et al. (2007). Cellular uptake of functionalized carbon nanotubes is independent of functional group and cell type. *Nature Nanotechnology*, *2*(2), 108–113.
11. Liu, Z., et al. (2007). In vivo biodistribution and highly efficient tumour targeting of carbon nanotubes in mice. *Nature Nanotechnology*, *2*(1), 47–52.
12. Liu, Y., et al. (2005). Polyethylenimine-grafted multiwalled carbon nanotubes for secure noncovalent immobilization and efficient delivery of DNA. *Angewandte Chemie (International ed. in English)*, *44*(30), 4782–4785.
13. Cheung, W., et al. (2010). DNA and carbon nanotubes as medicine. *Advanced Drug Delivery Reviews*, *62*(6), 633–649.
14. Zhang, Z., et al. (2006). Delivery of telomerase reverse transcriptase small interfering RNA in complex with positively charged single-walled carbon nanotubes suppresses tumor growth. *Clinical Cancer Research*, *12*(16), 4933–4939.
15. Varkouhi, A. K., et al. (2011). SiRNA delivery with functionalized carbon nanotubes. *International Journal of Pharmaceutics*, *416*(2), 419–425.
16. Zhao, D., et al. (2011). Carbon nanotubes enhance CpG uptake and potentiate antiglioma immunity. *Clinical Cancer Research*, *17*(4), 771–782.
17. Prakash, S., et al. (2011). Polymeric nanohybrids and functionalized carbon nanotubes as drug delivery carriers for cancer therapy. *Advanced Drug Delivery Reviews*, *63*(14–15), 1340–1351.
18. Hampel, S., et al. (2008). Carbon nanotubes filled with a chemotherapeutic agent: A nanocarrier mediates inhibition of tumor cell growth. *Nanomedicine*, *3*(2), 175–182.
19. Liu, Z., et al. (2007). Supramolecular chemistry on water-soluble carbon nanotubes for drug loading and delivery. *ACS Nano*, *1*(1), 50–56.
20. Bertucci, C., et al. (2006). Binding studies of taxanes to human serum albumin by bioaffinity chromatography and circular dichroism. *Journal of Pharmaceutical and Biomedical Analysis*, *42*(1), 81–87.
21. Kratz, F. (2008). Albumin as a drug carrier: design of prodrugs, drug conjugates and nanoparticles. *Journal of Controlled Release*, *132*(3), 171–183.
22. Liu, Z., et al. (2009). Preparation of carbon nanotube bioconjugates for biomedical applications. *Nature Protocols*, *4*(9), 1372–1382.
23. Lay, C. L., et al. (2010). Delivery of paclitaxel by physically loading onto poly(ethylene glycol) (PEG)-graft-carbon nanotubes for potent cancer therapeutics. *Nanotechnology*, *21*(6), 065101.
24. Ojima, I. (2008). Guided molecular missiles for tumor-targeting chemotherapy—case studies using the second-generation taxoids as warheads. *Accounts of Chemical Research*, *41*(1), 108–119.